

Large-Eddy Simulation of Starting Buoyant Jets

Ruo-Qian Wang¹, Adrian Wing-Keung Law², E. Eric Adams³, and Oliver B. Fringer⁴

¹Singapore-MIT Alliance for Research and Technology Center, S16-05-08, 3 Science Drive 2, Singapore 117543; PH (65) 6516-1171; FAX (65) 6778-5654; email: rwang@smart.mit.edu

²School of Civil and Environmental Engineering, Nanyang Technological University, Block N1 Rm 1a-03, 50 Nanyang Ave, Singapore 639798; PH (65) 6790-4104; FAX (65) 6791-0676; email: cwklaw@ntu.edu.sg

³Department of Civil and Environmental Engineering, Massachusetts Institute of Technology, Room 48-216b3, Cambridge, MA 02139; PH (617) 253-6595; FAX (617) 258-8850; email: eeadams@mit.edu

⁴Environmental Fluid Mechanics Laboratory, Stanford University, The Jerry Yang and Akiko Yamazaki Environment and Energy Building 473, Via Ortega, Office 187 Stanford, CA 94305; PH (650) 725-6878; FAX (650) 725-9720; email: fringer@stanford.edu

ABSTRACT

A series of Large Eddy Simulations (LES) is presented to investigate the penetration of starting buoyant jets. The LES code is first validated by comparing simulation results with existing experimental data for both steady and starting forced lazy plumes. The centerline decay and the growth rate of the steady state velocity and concentration fields, as well as the transient penetration rate, are found to compare well with the experiments. Then, the LES code is used to study the penetration of starting buoyant jets with buoyancies ranging from a pure jet to a lazy forced plume. The penetration rate is found to increase with an increasing buoyancy flux. It is also observed that, in the initial Period of Flow Development, the two penetrative mechanisms driven by the initial buoyancy and momentum fluxes are uncoupled.

INTRODUCTION

Buoyant jets are widely observed in nature as well as engineering applications. Most previous studies have focused on steady state behavior and the self-similar region (Fischer et al., 1979) rather than short-term and near-source behavior because of the complexity of source conditions, and limited understanding of the transition from jet-like to plume-like behavior. However, many buoyant jet applications are inherently short-term (e.g., the marine disposal of sediments from dredging or land reclamation), and even continuous discharges begin as starting jets or plumes. Hence the initial formation phase of buoyant jets is important.

Diez et al. (2003) used video techniques to study the characteristics of starting buoyant jets over a wide range of source buoyancy. Within the self-preserving phase, the plume was found to penetrate following the relationship of the $3/4$ power of time. Ai et al. (2006) performed experiments on a round starting forced plume using Particle Image Velocimetry (PIV) and Planar Laser Induced Fluorescence (PLIF), and covered a wide range of initial density differences from Boussinesq (relative density difference $\Delta\rho_0/\rho_0 < 15\%$) to non-Boussinesq ($\Delta\rho_0/\rho_0 > 15\%$) conditions. The paper provides an overview of the physics behind the intrusion of a starting round buoyant jet and the associated penetration rate. At the same time, they concluded that the complexities of the source condition as well as the details of the transition from jet-like to plume-like behavior need to be further investigated.

The above studies primarily used experimental tools to understand the starting buoyant jet phenomenon. By contrast, numerical simulations of starting buoyant jets are relatively rare. Iglesias et al. (2005) and Satti and Agrawal (2006, 2008) simulated helium jets injected into quiescent ambient air, motivated by the objective to improve the ignition of diesel engines. Satti and Agrawal (2008) showed that the penetration rate was strongly dependent on buoyancy; they further investigated the effect of buoyancy on developing buoyant jets, focusing on the details of the vortex ring evolution. Despite their pioneering effort, their study did not cover enough scenarios to allow a systematic analysis of the role of the buoyancy flux in the starting phenomenon.

The present study uses the Large-Eddy Simulation (LES) approach to examine the transient behavior of a starting buoyant jet in the initial Period of Flow Development (PFD). In particular, we aim to qualify the effect of buoyancy on the penetration rate based on the simulation results. Our work is part of a larger study to investigate the near-source transport of sediment released in coastal waters.

LES APPROACH

The governing equations for the LES approach are the spatially-filtered continuity, Navier-Stokes and scalar transport equations with the Boussinesq approximation. The governing equations are transformed to generalized curvilinear coordinates and discretized with a finite-volume formulation on a non-staggered grid (Zang et al., 1994). More details of the LES model can be found in Zang (1993). The numerical code has been validated by a series of comparisons with standard experiments (e.g. Zang 1993 and Cui and Street 2004) and shown to be a practical and efficient LES scheme that is suitable for turbulent flow simulations. The parallel version of the code that we use was developed by Cui and Street (2004).

The computational domain used in this study is a rectangular volume with a square horizontal cross-section that extends to $0.5 \text{ m} \times 0.5 \text{ m} \times 1.5 \text{ m}$ for validation, and $0.3 \text{ m} \times 0.3 \text{ m} \times 0.8 \text{ m}$ for the remaining production runs in the Cartesian coordinates of x , y and z respectively (as shown in Figure 1a). Note that the domain size is reduced

for the prediction runs so as to control the computational expense. At $t=0$, a buoyant jet with positive buoyancy (i.e. the buoyancy force is along the jet direction) is issued at a uniform velocity U_0 into a homogeneous and stationary ambient fluid with density ρ_0 . The normalized relative density difference between the jet flow and the ambient is $\Delta\rho_0/\rho_0$. The buoyant jet is discharged at the top of the domain through a circular nozzle which has a diameter $D=5$ cm. Thus the size of the domain can also be expressed as $10D \times 10D \times 30D$ and $6D \times 6D \times 16D$ for validation and production respectively, which shall limit the domain of investigation of the penetrative behavior. The computational domain is discretized into a stretched mesh with increased refinement along the vertical axis (see Figure 1b as an example).

The boundary conditions are also presented in Figure 1a. The velocity field is specified at the top boundary as an incoming uniform jet with a velocity field, for production runs, given by $w((x-3D)^2+(y-3D)^2 < D^2/4, z=0)=U_0$, while the other boundaries are all outflow boundaries. A constant volume flux, determined from the prescribed inflow velocity U_0 , was enforced at the inlet.

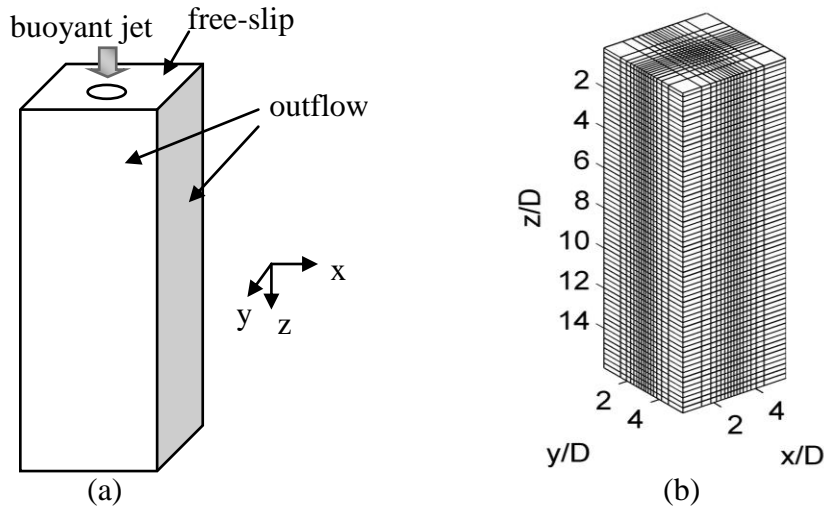


Figure 1 The computational domain: (a) boundary conditions (not to scale); (b) A typical grid mesh (only every 4th mesh point shown in each direction; the center of the jet outlet, for production runs, is at $x=3D, y=3D, z=0$)

VALIDATION

In this section, the LES model is validated for the study of buoyant jets by comparing the simulation results to experiments (Fischer et al., 1979; Ai et al., 2006; Wang and Law, 2002). Two types of validations are performed: (a) steady state and (b) starting phenomenon. In addition to the validation, the numerical simulations serve to optimize the required grid spacing.

In order to determine the penetration rate of a starting buoyant jet, it is necessary to pinpoint the tip of the penetrative front. We search for the tip at a particular time by scanning the concentration field layer by layer from the bottom towards the top of the computational domain. The first vertical position at which the threshold concentration is exceeded is determined to be the tip front.

Following is a validation study of a forced lazy plume whose characteristics are controlled by the initial buoyancy flux B_0 . For these simulations, the initial velocity U_0 was taken to be a small value of 0.05 m/s, while the reduced gravity $g\Delta\rho_0/\rho_0 = 0.7$ m/s². The corresponding Richardson number is $R_0 = (\pi/4)^{1/4} [g'D/U_0^2]^{1/2} = 3.49$ which lies within the lazy plume regime (Morton, 1959).

Figures 2 and 3 show that, using an averaging period of 40 s and a sampling frequency of 1 Hz, the axial velocity and concentration decay along the centerline become consistent beyond $t=40$ s. The fitting equation of Wang and Law (2002) successfully predicts the axial velocity decay beyond $z=6D$. One interesting aspect of the forced lazy plume is that the axial velocity increases very quickly in the laminar region near the source before decaying in the following turbulent self-similar region. The concentration decay is also well predicted with virtual origin correction, which assumes that a point source at $z=2.5D$ can properly represent the nozzle of a forced lazy plume (Hunt and Kaye, 2001). Note that the initial concentration remains constant in the laminar region until the approximate location where the velocity peaks. For the growth rate, Figure 4 and 5 show that the velocity and concentration (virtual origin corrected) spreading agree with values proposed by Wang and Law (2002) and Fischer et al. (1979), despite the fact that the equivalent radius narrows slightly in the potential core. It also appears that the center-line flow characteristics approach steady state earlier than the spreading width characteristics, which is somewhat expected, since axial flow development near the centerline of a jet or plume is dominant while the lateral development depends on the transverse turbulent shear dispersion and thus a larger time scale.

A numerical study on the dependence of grid size was conducted and the results are presented in Figure 6. They suggest that a grid mesh finer than $64 \times 64 \times 384$ is required for the penetration analysis. According to Figure 7 the non-dimensional penetration rate has a time power of 0.78 in the PDF, which is very close to the results of $3/4$ in Diez et al. (2003) and Ai et al. (2006). This comparison between the numerical and experimental studies validates the code for the simulations of the starting lazy plume. According to these validations and balancing the computational expense, grid meshes of $64 \times 64 \times 384$ are used for the following simulations.

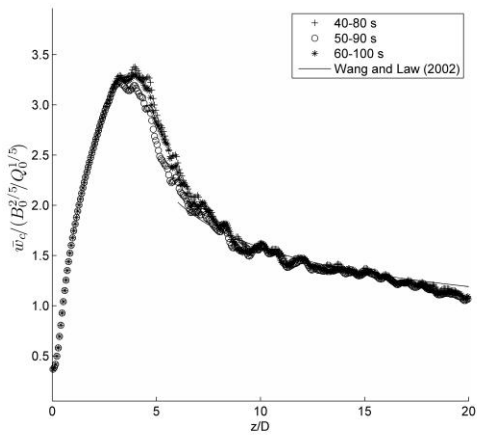


Figure 2 Mean axial velocity of forced lazy plume with different averaging periods.

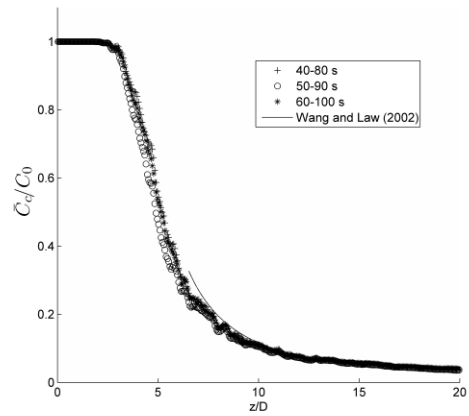


Figure 3 Mean axial concentration of forced lazy plume with different averaging periods.

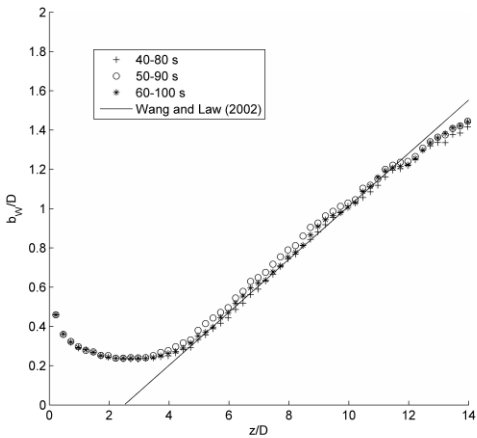


Figure 4 Mean velocity width of forced lazy plume with different averaging periods

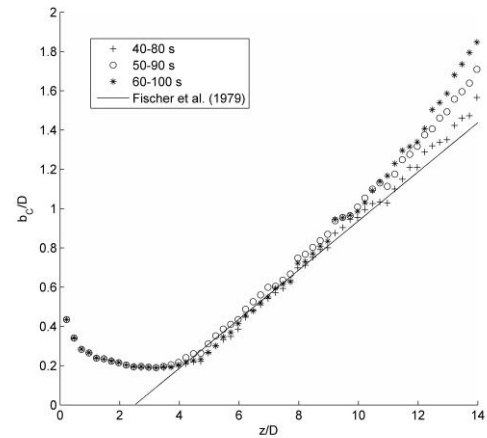


Figure 5 Mean concentration width of forced lazy plume with different averaging periods

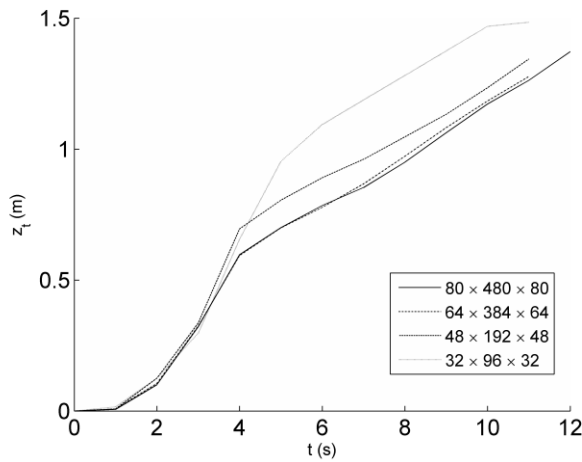


Figure 6 Penetration rate of forced lazy plume with different grids

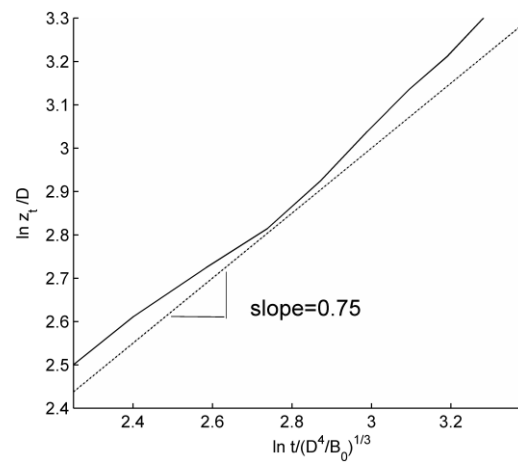


Figure 7 Dimensionless penetration rate of forced lazy plume

Validation of the steady and starting behavior of a pure jet was also performed. Results are omitted due to space limitations, but in general indicate favorable agreement between numerical simulations and experiments.

In summary, the present LES model performs credibly for the asymptotic cases of a pure jet and a lazy plume. Its transient performance is particularly convincing when simulations are compared with previous experimental data. The steady state results are also reliable and can be further improved if longer simulations are performed.

BUOYANT JET PENETRATION

3-D concentration distributions of a pure jet and a forced lazy plume at $t=3s$ are shown in Figures 8 and 9. A well organized mushroom-shape penetration head is present in the starting pure jet (Figure 8). For the plume (Figure 9), a sharper penetration head is found, where a bubble protrudes from the center of the penetration front to form a pear-shape head, differing from the flat one of the pure jet. The vortex ring has a smaller radius and the stem is significantly stretched. We can conclude that buoyancy flux significantly changes the shape of the penetration pattern.

The penetration rates of the pure jet and the forced lazy plumes are shown in Figure 10. Initially (until $tU_0/D=0.8$), all the fronts penetrate at the same rate. Afterwards, the pure jet penetrates linearly with time, whereas the forced lazy plumes penetrate much faster. When the lazy plume reaches the self-similar phases (e.g. for $R_0=1.768$ at $tU_0/D=6$), the penetration rates approach an asymptotic value as described above, i.e. $3/4$ of the square root of the time. According to these observations, the development of the penetration rates for buoyant plumes can be divided into three phases: the initial phase where penetration overlaps that of a pure jet, the middle accelerated phase, and the last asymptotic phase. To isolate the effects of buoyancy flux, simulations were performed for buoyant jets with several different values of initial buoyancy, characterized by the discharge Richardson number, R_0 . The penetration distance of the pure jet ($R_0 = 0$) is subtracted from the penetration of the other buoyant jets, and the excess penetration distances are shown versus time in Figure 11. For comparison, excess penetration distances of plumes with different initial momentum fluxes (i.e. Reynolds numbers) are shown in the same figure.

The formation of the three phases of the penetration rate can be interpreted by the balance of the two driving mechanisms, i.e. the initial momentum flux and the buoyancy inducement. In the initial overlapped phase, the buoyancy flux has no time to significantly accelerate the penetration. Therefore, the momentum flux dominates the driving force and the penetration distances overlap each other. In the middle accelerated phase, the potential energy contained in the buoyancy flux is transformed by gravitational acceleration to kinetic energy. Thus, the penetration rate is accelerated as shown in Figure 10. Figure 11 isolates the buoyancy effects from the initial momentum in terms of excess penetration distance. For the same density difference but different initial momentums, the penetration distances are found to

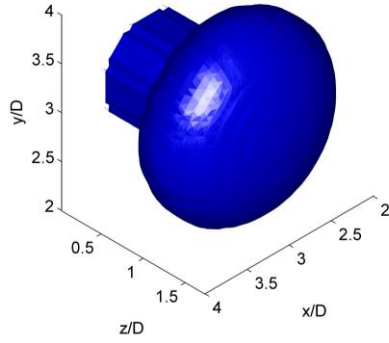


Figure 8 Isosurface of density ($\rho/\rho_0=0.3\Delta\rho_0/\rho_0$) for a pure jet ($Re=2500, R_0=0$)

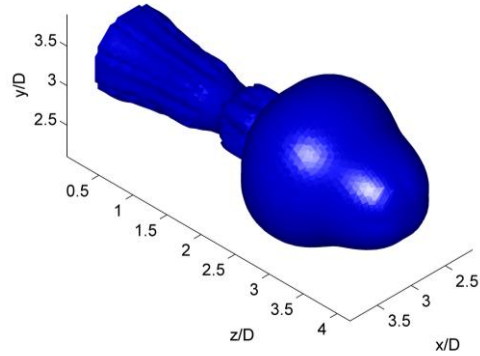


Figure 9 Isosurface of density ($\rho/\rho_0=0.3\Delta\rho_0/\rho_0$) for a forced lazy plume ($Re=2500, R_0=1.768$)

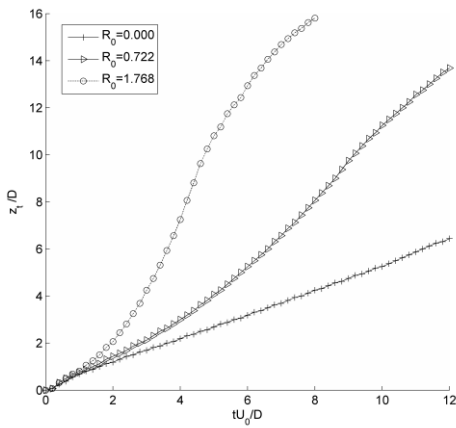


Figure 10 The penetration of buoyant jets in the PFD under different buoyancy fluxes

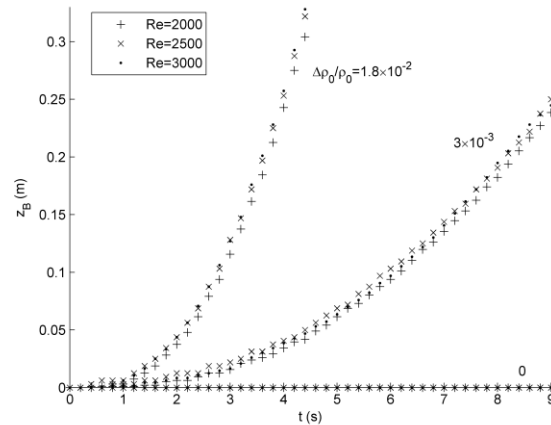


Figure 11 The excess penetration induced by buoyancy flux

overlap each other. This suggests that the total penetration distance can be resolved as the addition of the penetration effects driven by initial momentum and the buoyancy flux separately. Because these two factors are uncoupled, the relationship between them appears to be linear. Finally, in the last self-similar phase (or PDF), the total penetration rate is decreased due to the greater entrainment of ambient fluid. At the same time, the momentum flux and buoyancy inducement interact nonlinearly with each other and result in the asymptotic advancing principle of $3/4$ power of time. These simulations and their analysis will allow us to quantify the combined effects of buoyancy and momentum on frontal penetration rates within PFD (forthcoming).

SUMMARY AND CONCLUSIONS

A numerical study using LES has been conducted to investigate the penetration behavior of a starting buoyant jet during the PFD. Known behavior of the two

asymptotic cases of a lazy plume (shown) and a pure jet (not shown) have been reproduced to validate the numerical code. The steady-state results of the centerline decay and the growth rate of concentration and velocity fields compare favorably with the experimental data reported in the literature. The corresponding transient simulations are also consistent with the experiments reported previously.

After the validation, the model is used to simulate starting turbulent buoyant jets with a comparison between a force lazy plume and a pure jet. The buoyancy flux significantly changes the shape of the penetration head, and the penetration front advances faster with buoyancy. The penetrative distances induced by the initial buoyancy fluxes and by the initial momentum fluxes are found to be independent; therefore, the total penetration distance can be treated as a linear combination of these two parts. Quantitative results concerning the combined penetration are forthcoming.

ACKNOWLEDGEMENT

This work was supported by Singapore's National Research Foundation through the Singapore-MIT Alliance for Research and Technology.

REFERENCES

- Ai, J.J., Law, A.W.K., Yu, S.C.M. (2006). "On Boussinesq and non-Boussinesq starting forced plumes." *J. Fluid Mechanics*, 558, 357-386.
- Cui, A., Street, R.L. (2004). "Large-Eddy Simulation of Coastal Upwelling Flow." *Environmental Fluid Mechanics*." 4(2), 197-223.
- Diez, F. J., Sangras, R., Faeth, G.M., Kwon, O.C. (2003). "Self-preserving properties of unsteady round buoyant turbulent plumes and thermals in still fluids." *Transactions of the ASME. Journal of Heat Transfer*, 125(5), 821-851.
- Fischer, H.B., List, E.J., Koh, R.C.Y., Imberger, J., Brooks, N.H. (1979). *Mixing in inland and coastal waters*, New York: Academic Press.
- Hunt, G.R., Kaye, N.G. (2001). "Virtual origin correction for lazy turbulent plumes." *J. Fluid Mechanics*, 435:377-396
- Iglesias, I., Vera, M., Sánchez, A.L., Liñán, A. (2005). "Simulations of starting gas jets at low Mach numbers." *Physics of Fluids*, 17(3), 38105-38109.
- Morton, B.R. (1959). "Forced plumes." *Journal of Fluid Mechanics*, 5, 151-163.
- Satti, R.P., Agrawal, A.K. (2006). "Computational analysis of gravitational effects in low-density gas jets." *AIAA Journal*, 44(7), 1505-1515.
- Satti, R.P., Agrawal, A.K. (2008). "Computational study of buoyancy effects in a laminar starting jet." *In 'll Journal of Heat and Fluid Flow*." 29(2), 527-539.
- Wang, H., Law, A.W.K. (2002). "Second-Order Integral Model for a Round Turbulent Buoyant Jet." *Journal of Fluid Mechanics*, 459, 397-428.
- Zang, Y. (1993), *On the Development of Tools for the Simulation of Geophysical Flows*, PhD thesis, Stanford University, Stanford, CA
- Zang, Y., Street, R., Koseff, J. (1994). A non-staggered grid, fractional step method for time-dependent incompressible Navier-Stokes equations in curvilinear coordinates. *Journal of Computational Physics*, 114(1), 18-33.